Proceedings of the
Annual Stability Conference
Structural Stability Research Council
Atlanta, Georgia, April 21-24, 2026

Assessment of AISC 360 column design curve using flexural buckling simulations of high-strength steel columns

Shahriar Quayyum[1], Ronald D. Ziemian[2], Constance W. Ziemian[3]

Abstract

The flexural buckling behavior of structural steel columns fabricated from high-strength steel (specified yield strength 65 ksi or above) is investigated, comparing the performance of wide-flange (W) shapes and hollow structural sections (HSS) under axial compression. Nonlinear finite element models accounting for initial geometric imperfections (out-of-straightness), shape-specific residual stress distributions, and nonlinear material behavior are developed and validated against experimental results from benchmark studies. A comprehensive parametric study across various cross-sectional geometries, which includes both W-shapes and HSS, and a range of slenderness ratios covering both inelastic and elastic buckling regimes is then conducted to generate compressive strength curves for both major-axis and minor-axis buckling.

The numerically derived strength curves are compared with the current column design provisions in AISC 360 to evaluate their accuracy and conservatism for high-strength steels. Results indicate that the present design method tends to underestimate the capacity of high-strength W-shape and HSS columns. This conservatism stems largely from residual stress and imperfection assumptions calibrated on lower-strength steels. The findings support discussion on whether a unified column curve is sufficient or whether distinct design curves should be adopted based on section type (e.g., W-shape vs. HSS) and yield strength level. The study offers recommendations that could inform future updates to the AISC 360 Specification and other design standards to better accommodate the behavior of high-strength steel columns.

1. Introduction

The use of high-strength structural steel in compression members has gained increasing attention due to its potential to reduce member size, structural weight, fabrication demands, and embodied carbon, particularly in gravity-dominated and compression-controlled structural systems (AISC 2019). Advances in steel production, including quenching and self-tempering (QST) processes, have enabled the manufacture of rolled wide-flange (W) sections with specified yield strengths up to 80 ksi, such as ASTM A913 Grade 80 (ASTM A913/A913M). High-strength steel is also increasingly used in hollow structural section (HSS) columns, especially in applications where

[1] Assistant Professor, Manhattan University, <shahriar.quayyum@manhattan.edu>
[2] Professor, Bucknell University, <ziemian@bucknell.edu>
[3] Professor, Bucknell University, <cziemian@bucknell, edu>

architectural constraints, durability, or biaxial performance govern design (Wang and Gardner 2013, Somodi and Kövesdi 2016, 2017). Despite these developments, the adoption of high-strength steel columns in building structures remains limited, in part due to uncertainty regarding the applicability of existing column stability provisions to modern materials and cross-sectional shapes (Stall *et al*. 2024).

Current column design provisions in AISC 360-22 are based on a single unified column curve calibrated primarily using experimental and analytical data for conventional mild steels and rolled W-shapes (AISC 2022). The development of this curve, rooted in decades of research is summarized in the *SSRC Guide to Stability Design Criteria for Metal Structures* (Ziemian 2010), reflects assumed levels of initial geometric imperfections and residual stresses representative of rolling and fabrication practices prevalent at the time of calibration (Galambos and Ketter 1959, Bjorhovde 1972, Fukumoto and Itoh 1983). While this unified approach has proven robust and conservative for conventional steels, its applicability to modern high-strength steel columns - particularly across different cross-section types - has not been comprehensively evaluated.

A substantial body of research has investigated the flexural buckling behavior of high-strength steel columns, with much of the work focused on welded, built-up, or cold-formed members. Experimental and numerical studies on welded I-sections, box sections, and built-up members fabricated from steels such as S690 and S960 have consistently demonstrated that Eurocode 3 buckling curves tend to underestimate buckling resistance for high-strength steels (Rasmussen and Hancock 1995, Li *et al*. 2012, Ban *et al*. 2013, Ma *et al*. 2015, Sun *et al*. 2020, Ferreira Filho *et al*. 2022). In contrast, AISC provisions generally provide closer, though still variable, predictions depending on section geometry and slenderness range (Wang and Gardner 2013, Yun *et al*. 2023). These studies have shown that residual stress magnitudes do not scale proportionally with yield strength and that higher-strength steels may exhibit improved normalized buckling performance relative to existing curves, particularly in the inelastic slenderness range (Boissonnade and Somja 2012, Jönsson and Stan 2017).

High-strength hollow structural section (HSS) columns, including both cold-formed and hot-finished sections, have also been investigated in prior research. Closed sections generally exhibit reduced sensitivity to geometric imperfections, more uniform stress flow, and improved global stability relative to open sections (Wang and Gardner 2013, Somodi and Kövesdi 2016). Experimental and numerical studies on high-strength circular and square HSS columns have reported buckling strengths that meet or exceed predictions from existing design curves, although their behavior is influenced by cold-forming residual stresses, local buckling characteristics, and cross-sectional slenderness (Somodi and Kövesdi 2017, Stroetmann *et al*. 2024). Importantly, the stability behavior of HSS columns differs fundamentally from that of rolled W-shapes, and results obtained for one cross-section type cannot be directly transferred to another.

Rolled W-shapes exhibit residual stress distributions governed primarily by the nonuniform cooling process following hot rolling. Numerous studies have shown that residual stresses in rolled shapes are strongly dependent on section size and geometry and do not increase in proportion to yield strength (Alpsten 1968, Huber 1956, Lamarche and Tremblay 2011). Larger rolled sections, in particular, tend to develop higher compressive residual stresses in the flanges due to slower cooling rates, which can reduce flexural buckling resistance in the inelastic range and promote

early local instability (ECCS TC8 2008, Quayyum and Hassan 2017). These effects are not explicitly reflected in the unified AISC column curve, which assumes idealized residual stress patterns based on historical data for conventional steels (Galambos and Ketter 1959).

Design standards differ in how they account for these effects. Eurocode 3 addresses variability in residual stresses and imperfection sensitivity through multiple buckling curves based on fabrication method and cross-section type (EN 1993-1-1 2005), whereas AISC 360 adopts a single unified curve for simplicity and conservatism (AISC 2022). Notably, AISC 370 introduces shape-specific column curves for stainless steel structures, explicitly recognizing the influence of cross-section geometry on flexural buckling behavior (AISC 2021). This precedent demonstrates that shape-dependent stability treatment can be incorporated within the AISC framework when warranted by material behavior.

Taken together, prior research indicates that flexural buckling behavior of steel columns is influenced by a complex interaction of material strength, residual stresses, geometric imperfections, cross-section shape, and buckling axis. While existing design provisions provide a reliable baseline for conventional materials and sections, their applicability to high-strength steel columns - particularly across different cross-sectional shapes - remains an open question.

Accordingly, this study investigates the flexural buckling behavior of high-strength steel columns across three common cross-section types: rolled wide-flange, circular hollow structural section (HSS), and square HSS. Validated nonlinear finite element models incorporating residual stresses, initial geometric imperfections, and nonlinear material behavior are employed to develop column buckling curves over a broad range of geometries and slenderness ratios. The resulting buckling responses are compared with current AISC 360 and Eurocode 3 provisions to clarify the influence of cross-section geometry and material strength on column stability and to assess the adequacy of existing unified column curve formulations for high-strength steel applications.

2. Finite Element Modeling Framework

2.1 General Modeling Approach

Three-dimensional nonlinear finite element (FE) models are developed to investigate the flexural buckling behavior of high-strength steel columns, including rolled wide-flange (W), circular HSS, and square HSS sections as shown in Figure 1a. The analyses are performed using ANSYS (ANSYS 2023) and incorporate geometric and material nonlinearities, initial geometric imperfections, and residual stresses. The modeling approach is intended to capture global flexural buckling behavior and associated post-buckling response.

2.2 Geometry, Boundary Conditions, and Element Selection

All columns are modeled as prismatic members with simply supported end conditions (Figure 1b) and discretized using 20-node solid elements (SOLID186). For rolled W-shapes, fillet regions are omitted, and section properties are computed without the k-area. The column longitudinal axis is aligned with the global x-axis, with the y- and z-axes lying in the cross-sectional plane. Boundary conditions are applied to isolate major- and minor-axis buckling for W-shapes. For major-axis buckling, minor-axis displacements are restrained along the column length. Circular and square

HSS columns are modeled with bending about a principal axis. Representative meshes and boundary conditions are shown in Figure 1.

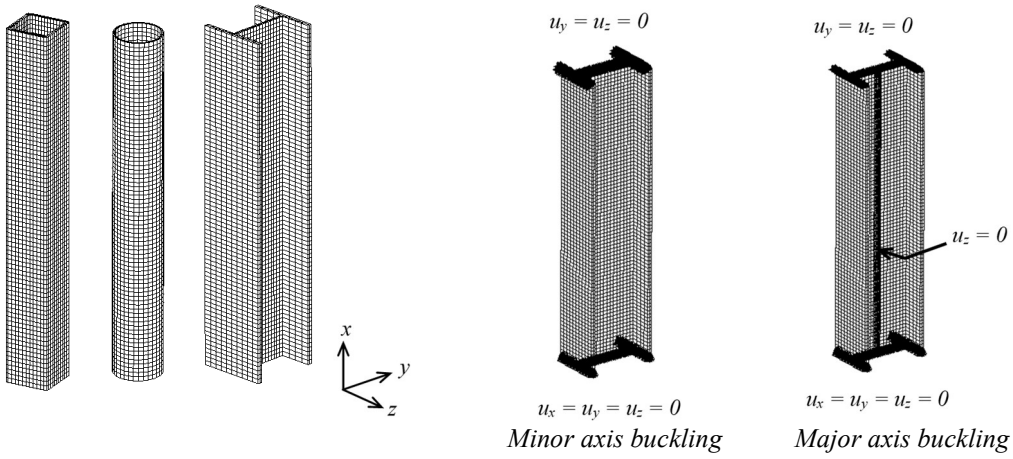

(a) FE mesh

(b) Boundary conditions applied in W-shapes

Figure 1: (a) FE meshes for W shape and HSS column sections, (b) boundary conditions for minor and major axis buckling of W-shape.

2.3 Material Modeling

Nonlinear material behavior is represented using a multilinear kinematic hardening plasticity model. ASTM A992 steel is characterized by a yield plateau and extended strain hardening (Figure 2a), while ASTM A913/A913M Grade 80 steel exhibits a smooth elastic - plastic transition with limited strain hardening (Figure 2b). An elastic modulus of 29,000 ksi is adopted for both steels. Material parameters are calibrated using uniaxial tension test data reported by Morrison (2015) for A992 steel and coupon tests provided by one of the producers for A913 Grade 80 steel.

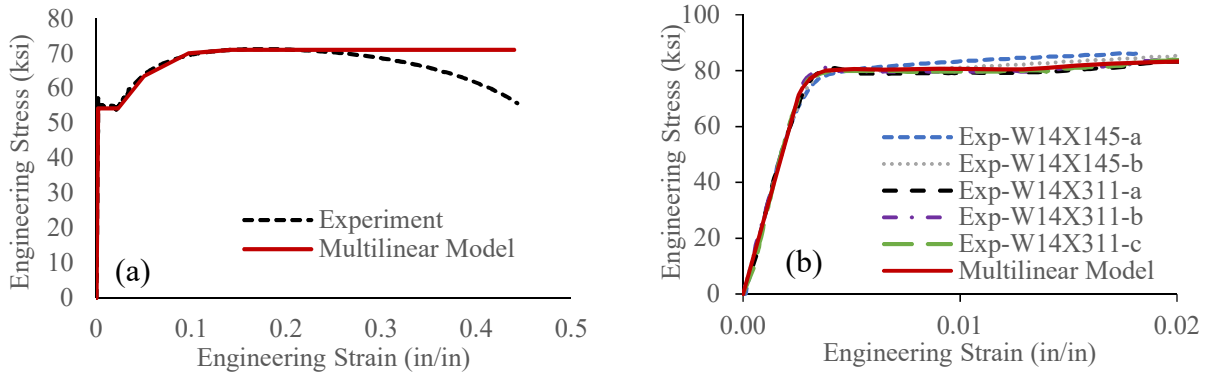

Figure 2: Experimental uniaxial tension data and fitted true stress–strain material models for (a) A992 and (b) A913 Grade 80 steels.

Cold-formed circular and square HSS columns are modeled using ASTM A500 Grade C material properties, with S700 steel adopted as a surrogate for high-strength HSS due to the limited availability of U.S.-based experimental data for higher-strength cold-formed sections. The nonlinear material models developed in this study are based on experimental stress–strain data reported by Meng and Gardner (2021) for S700 circular hollow sections (CHS) and by Yin *et al*.

(2024) for S700 square hollow sections (SHS). ASTM A500 Grade C material properties are obtained from the study by Fabben and McCormick (2014) for square HSS and from the experimental investigation by Voth and Packer (2012) for circular HSS. The resulting models capture the elastic modulus, yield strength, smooth elastic-plastic transition, and limited ductility characteristic of both conventional and high-strength cold-formed HSS steels as shown in Figures 3 and 4, respectively.

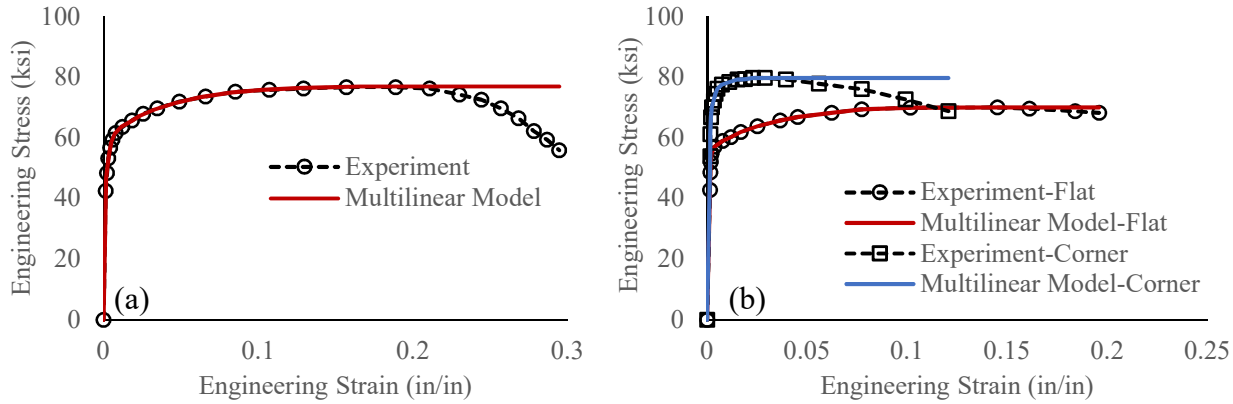

Figure 3: Experimental uniaxial tension data and corresponding fitted stress–strain material models for A500 Gr. C (a) CHS and (b) SHS used in the finite element analyses.

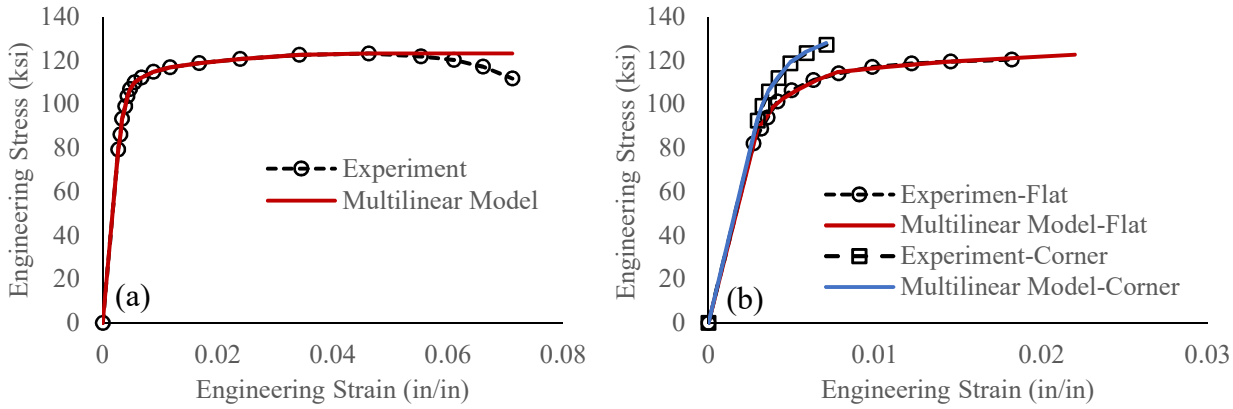

Figure 4: Experimental uniaxial tension data and corresponding fitted true stress–strain material models for S700 (a) CHS and (b) SHS used in the finite element analyses.

2.4 Initial Geometric Imperfections

Initial geometric imperfections are introduced based on the lowest elastic buckling mode obtained from linear eigenvalue analysis. The imperfection amplitude is taken as L/1500, consistent with the assumptions underlying the SSRC column curves and the AISC 360 unified column curve. The normalized buckling mode is scaled to the prescribed amplitude and superimposed onto the perfect geometry prior to nonlinear analysis as shown in Figure 5.

2.5 Modeling of Residual Stresses

Residual stresses in rolled W-shapes are explicitly incorporated as initial stress states obtained from a validated sequentially coupled thermo-mechanical analysis simulating the cooling process after hot rolling (Quayyum and Hassan 2017). The analysis captures nonuniform cooling, phase transformation effects, and temperature-dependent material properties. The predicted residual

stress distributions are validated against measured data for A992 W12×87 and A913 Grade 80 W14×808 sections (Lamarche and Tremblay 2011, Spoorenberg *et al*. 2013) as shown in Figures 6 and 7, respectively. The residual stresses predicted by the model proposed by Galambos and Ketter (1959) are also plotted in Figures 6 and 7 for comparison purposes.

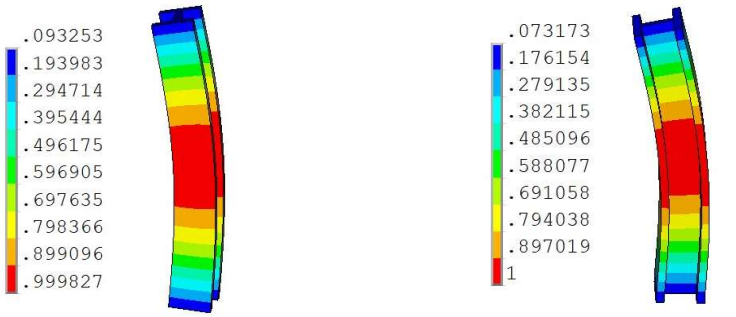

(a) Minor axis (b) Major axis

Figure 5: Normalized displacements of the lowest global buckling mode from elastic buckling analysis.

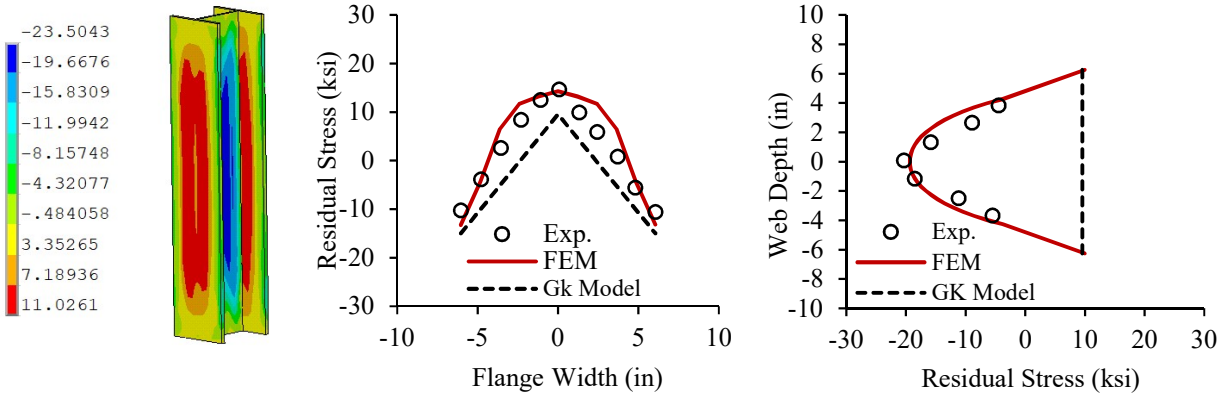

Figure 6: Measured and simulated longitudinal residual stress distribution in ASTM A992 W12×87 beam section (data from Lamarche and Tremblay 2011).

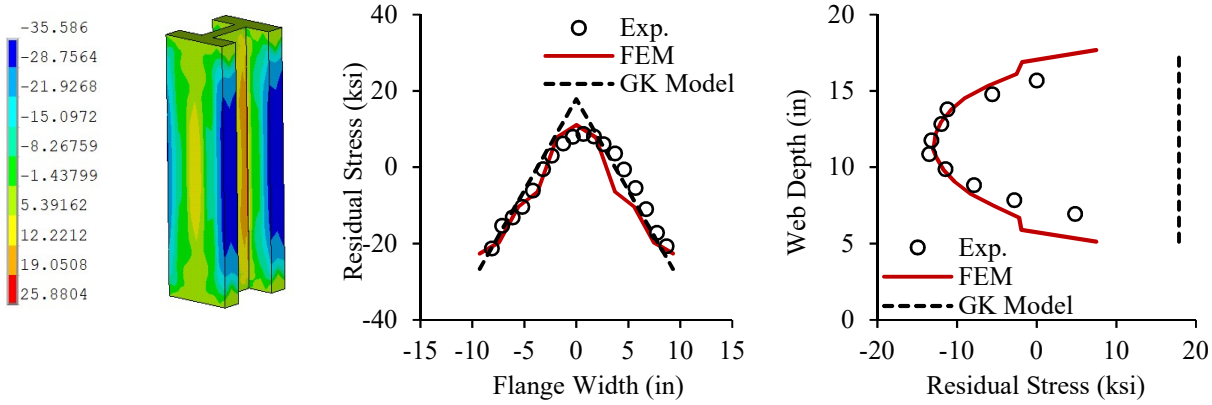

Figure 7: Measured and simulated longitudinal residual stress distribution in 80 ksi W14×808 beam section (data from Spoorenberg *et al*. 2013).

For cold-formed circular and square HSS columns, residual stresses arising from forming processes are not explicitly simulated. Residual stress distributions for circular and square HSS columns are adopted from the shape-specific residual stress models provided in EN 1993-1-14 (2020), which summarizes experimentally informed residual stress patterns for cold-finished CHS and RHS sections. Although originally developed for carbon steel grades, these normalized distributions are expressed relative to yield strength and are therefore adopted herein for high-strength HSS as a rational approximation in the absence of U.S.-based measurements. These distributions are implemented as self-equilibrated initial stress fields consistent with the fabrication process and cross-section geometry. While these residual stress assumptions are necessarily idealized, validation studies as summarized in Section 2.6 confirmed that the adopted modeling approach accurately captures global flexural buckling behavior.

2.6 Validation of the Modeling Framework

The FE modeling framework is validated against experimental results for a W12×87 column tested under monotonic axial compression (Lamarche and Tremblay 2011). Simulations incorporating both residual stresses and initial imperfections accurately reproduce the observed buckling mode, load-displacement response, and post-buckling behavior as shown in Figure 8. Analyses neglecting residual stresses overpredict buckling strength by approximately 10%, confirming the importance of explicitly modeling residual stresses. In addition, the finite element models developed for circular and square HSS columns are validated against experimental results reported by Meng and Gardner (2021) for CHS and by Yin *et al*. (2024) for SHS. The simulations capture the reported buckling modes and normalized buckling strengths with good agreement (Figure 9), providing confidence in the applicability of the modeling framework across different cross-section types. The validated framework is subsequently used to develop flexural buckling curves for rolled W shape and HSS columns fabricated from high-strength steel.

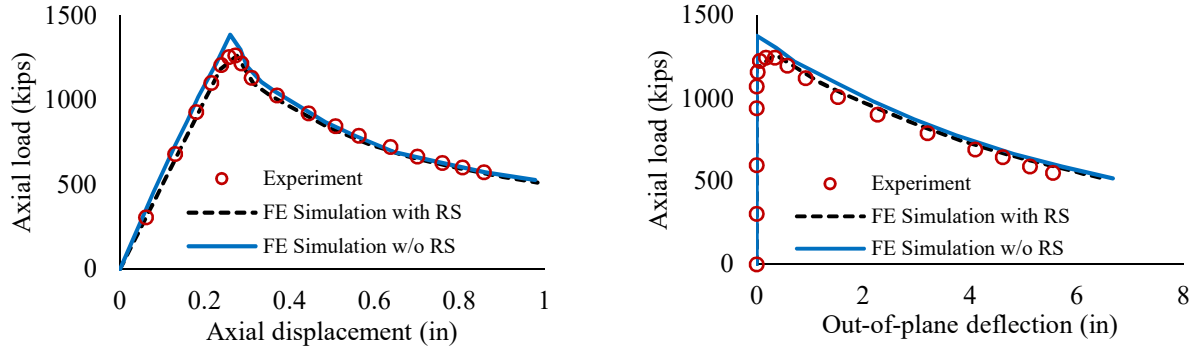

(a) Axial load-displacement

(b) Axial load-lateral deflection

Figure 8: Buckling analysis vs. experimental (data from Lamarche and Tremblay 2011) responses under monotonic axial loading for ASTM A992 W12×87 section.

3. Flexural Buckling Response of W-Shape Columns

A representative set of rolled W-shape sections fabricated from ASTM A992 (F_y = 50 ksi) and ASTM A913 Grade 80 (F_y = 80 ksi) steels is analyzed, as summarized in Table 1. The selected sections span a wide range of flange thicknesses, width-to-thickness ratios, and radii of gyration to capture the influence of section geometry on flexural buckling behavior. All selected W-shapes satisfy the AISC 360 width-to-thickness limits for compression elements evaluated using the corresponding yield strengths; therefore, none of the sections are classified as slender, and local

buckling is not expected to govern the response. Column lengths are varied to cover nondimensional slenderness ratios extending from the inelastic buckling regime through the elastic buckling range. Buckling strengths are presented in normalized form as the ratio of critical buckling stress to yield stress (F_{cr}/F_y) plotted against nondimensional slenderness λ given as:

$$\lambda = \frac{1}{\pi}\frac{L_c}{r}\sqrt{\frac{F_y}{E}} \quad (1)$$

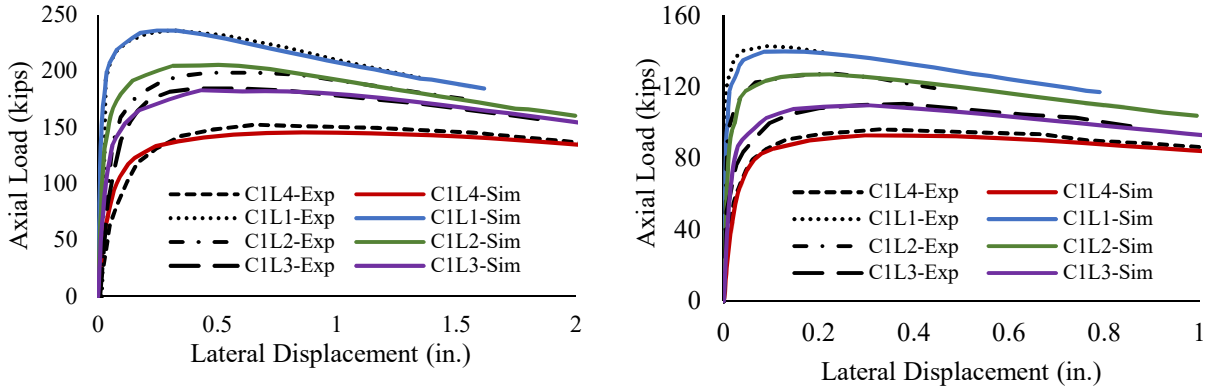

(a) CHS (Meng and Gardner 2021)

(b) SHS (Yin *et al*. 2024)

Figure 9: Buckling analysis vs. experimental responses under monotonic axial loading for S700 HSS sections.

Table 1: Cross-sectional properties of the W-shape columns investigated for flexural buckling

Column Designation	h/b	t_f (in.)	$b_f/2t_f$	h/t_w
W14×808	1.23	5.12	1.82	3.04
W14×605	1.20	4.16	2.09	4.39
W14×500	1.15	3.50	2.43	5.21
W14×426	1.12	3.04	2.75	6.08
W14×342	1.07	2.47	3.31	7.41
W14×257	1.03	1.89	4.23	9.71
W14×211	1.00	1.56	5.06	11.6
W14×193	0.99	1.44	5.45	12.8
W14×176	0.97	1.31	5.97	13.7
W14×145	0.96	1.09	7.11	16.8
W14×132	1.00	1.03	7.15	17.7
W14×120	0.99	0.94	7.80	19.3
W14×90	0.97	0.71	10.2	25.9
W14×82	1.41	0.855	5.92	22.4
W14×68	1.40	0.72	6.97	27.5
W12×87	1.03	0.81	7.48	18.9
W12×336	1.25	2.96	2.26	5.47

3.1Major- and Minor-Axis Buckling Trends

For both A992 and A913 Grade 80 steels, the simulated major-axis buckling curves closely follow the AISC 360 column curve at low slenderness ($\lambda < 0.5$), where yielding governs, and at high slenderness ($\lambda > 1.5$), where elastic Euler buckling controls (Figure 10). In these regimes, differences between numerical results and AISC predictions are generally within ±3%. In the intermediate, inelastic buckling range (approximately $0.5 \leq \lambda \leq 1.5$), systematic deviations emerge as evident from Figure 9. For A992 sections, major-axis buckling strengths exceed the AISC curve

by approximately 5-10% for light-to-moderate sections, while heavier sections show closer agreement. For A913 Grade 80 sections, the upward shift relative to AISC predictions is more pronounced. Depending on section geometry, simulated major-axis buckling strengths are approximately 5–14% higher than the AISC 360 curve, with the largest increases observed for sections with h/b < 1.12 and flange thickness t_f < 3 in. Heavy sections with thick flanges ($t_f \geq 3$ to 4 in.) show smaller increases on the order of 3–8%, reflecting the growing influence of compressive residual stresses.

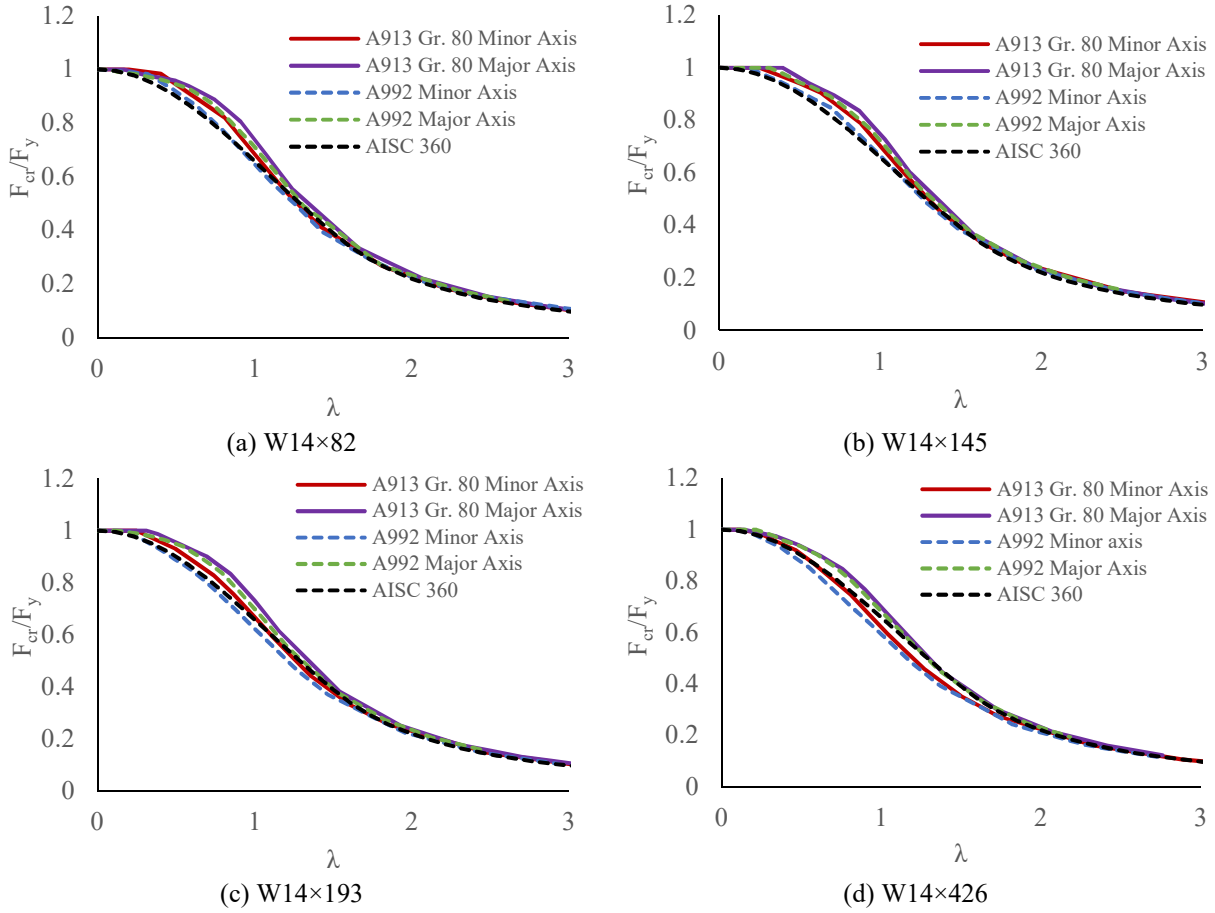

Figure 10: Simulated column flexural buckling curves for W-shapes using A913/913M Gr. 80 and A992 steels.

Across all cases, major-axis buckling strengths consistently exceed minor-axis strengths, indicating that the use of a single unified curve for both axes can be conservative for major-axis buckling, particularly for high-strength rolled sections. Minor-axis buckling exhibits greater sensitivity to section geometry and residual stress magnitude. For A992 columns, the AISC 360 curve provides good agreement for non-heavy sections (t_f < 1.5 in., $b_f/2t_f \geq 5.5$), while overestimating buckling resistance by up to about 12% for heavy sections with thick flanges in the inelastic range ($0.5 \leq \lambda \leq 1.5$). This behavior is directly linked to larger compressive residual stresses in the flanges of large rolled shapes. For A913 Grade 80 columns, two distinct trends are observed. For compact and moderately proportioned sections (h/b < 1.12, t_f < 3 in.), simulated minor-axis buckling strengths exceed AISC predictions by approximately 4–11% over much of the inelastic range. In contrast, for very heavy sections with large flange thicknesses, the AISC curve slightly overpredicts buckling strength, typically by 2-8%, due to the disproportionate

increase in compressive residual stresses relative to yield strength. Eurocode 3 buckling curves are consistently more conservative than AISC 360 for both steels and both buckling axes. While EC3 captures geometry-dependent trends through multiple curves, it underestimates buckling resistance for most of the W-shapes considered, particularly for high-strength steel in the inelastic range.

3.2 Comparison with AISC 360 and Eurocode 3

Direct comparisons with the AISC 360 column curve (Figure 11) demonstrate that the unified curve provides a reasonable lower-bound estimate for W-shape columns across a broad range of cases. However, the degree of conservatism varies with section geometry and yield strength. For several A913 Grade 80 W-shapes, the numerical buckling strengths exceed AISC predictions by a modest margin in the inelastic buckling regime. Comparisons with Eurocode 3 further highlight differences in design philosophy and imperfection modeling.

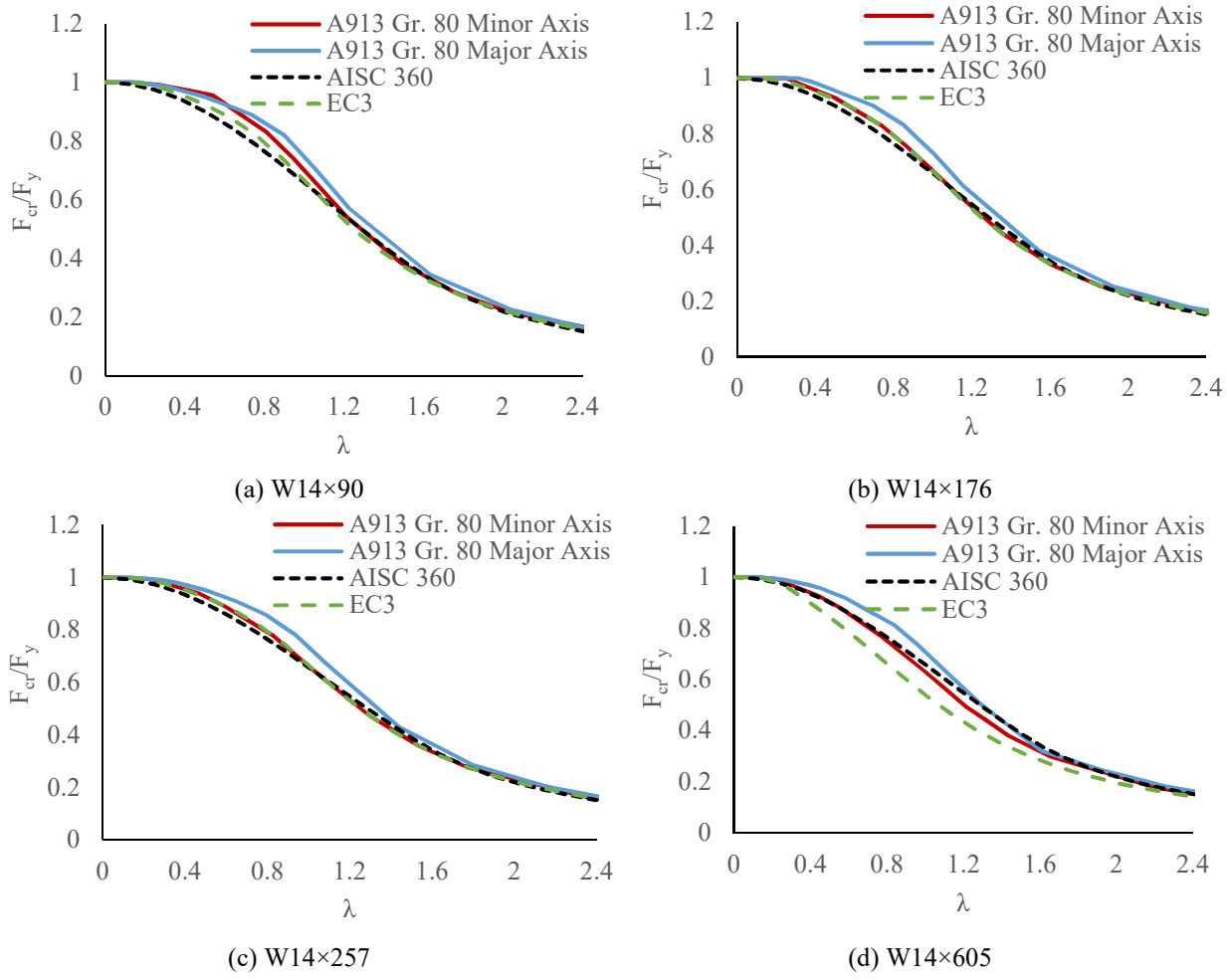

(a) W14×90

(b) W14×176

(c) W14×257

(d) W14×605

Figure 11: Comparison of column flexural buckling curves for A913/A913M Gr. 80 steel W-shapes with AISC 360 and Eurocode 3.

For the W-shape columns examined, Eurocode 3 buckling curves are consistently more conservative than AISC 360 predictions, particularly for high-strength steel. For ASTM A913 Grade 80 sections, Eurocode predictions are typically 10–20% lower than the numerically simulated buckling strengths in the inelastic range, reflecting the larger imperfection factors and

calibration basis of the Eurocode framework. Although Eurocode 3 accounts for fabrication effects through multiple buckling curves, its provisions appear overly conservative for modern rolled high-strength wide-flange sections. Overall, the comparison confirms that the AISC 360 unified column curve provides a reasonable lower-bound estimate for rolled wide-flange columns across a wide range of cases, but with conservatism that depends on buckling axis, section geometry, and yield strength. The wide-flange results also confirm that the numerical modeling framework captures expected flexural buckling trends and provides a consistent and validated reference for subsequent evaluation of circular and square HSS column behavior.

4. Flexural Buckling Response of Hollow Structural Section (HSS) Columns

This section extends the numerical investigation to hollow structural section (HSS) columns to examine how closed-section geometry influences flexural buckling behavior at high yield strengths. Unlike open W-shapes, HSS columns exhibit closed-section behavior that affects stiffness distribution, stress redistribution, imperfection sensitivity, and residual stress development. Despite the widespread use of HSS columns in practice, publicly available material data for high-strength HSS produced in the United States are limited, particularly for yield strengths exceeding 65 ksi. To address this limitation, S700 European structural steel was adopted in this study as a representative high-strength material. The use of S700 steel enables a parametric investigation of high-strength HSS buckling behavior without implying direct applicability to current U.S. design specifications. The intent of this investigation is to identify trends in buckling response and to evaluate the adequacy of the AISC 360 column curve when applied to closed-section columns at high yield strength levels. Both circular hollow sections (CHS) and square hollow sections (SHS) were considered. The selected sections span a range of diameter-to-thickness and width-to-thickness ratios representative of practical HSS geometries as summarized in Table 2. All HSS sections modeled using S700 material properties and ASTM A500 Gr. C steel, satisfy the AISC 360 width-to-thickness limits for non-slender compression elements; accordingly, local buckling is not expected to govern the response. Column lengths were varied to cover inelastic and elastic buckling regimes consistent with the W shape study.

Table 2: Cross-sectional properties of S700 HSS columns investigated for flexural buckling

Round HSS Column Designation	***D/t***	***t (in)***	**Square HSS Column Designation**	***b/t or h/t***	***t (in)***
HSS10×0.375	28.7	0.349	HSS5×5×0.25	18.5	0.233
HSS10×0.5	21.5	0.465	HSS5×5×0.312	14.2	0.291
HSS10×0.625	17.2	0.581	HSS5×5×0.375	11.3	0.349
HSS5×0.375	14.3	0.349	HSS5×5×0.5	7.75	0.465
HSS5×0.5	10.8	0.465	HSS4×4×0.5	5.60	0.465
HSS7.5×0.5	16.1	0.465	HSS6×6×0.5	9.90	0.465
HSS12×0.5	16.9	0.465	HSS8×8×0.5	14.2	0.465
HSS14×0.5	30.1	0.465	HSS10×10×0.5	18.5	0.465

4.1 Buckling Response of Circular HSS Columns

The normalized buckling curves for circular HSS columns (Figure 12a) indicate that the AISC 360 unified column curve consistently underestimates buckling strength in the inelastic slenderness range. For most CHS sections considered, the numerical curves lie approximately 5–10% above the AISC curve for $0.5 \leq \lambda \leq 1.50$. As slenderness increases and elastic buckling becomes dominant, the numerical results gradually converge toward the AISC curve, reflecting reduced sensitivity to

residual stresses and material nonlinearity. The relatively tight clustering of the CHS curves demonstrates limited sensitivity to section slenderness and diameter-to-thickness ratio within the practical range examined. Compared with W-shape columns, circular HSS columns exhibit buckling behavior comparable to or slightly stronger than W-shape columns buckling about the major axis (Figure 12c). This behavior is attributed to the axisymmetric, closed geometry of CHS members, which promotes uniform stress redistribution and reduces sensitivity to both initial geometric imperfections and residual stresses.

4.2 Buckling Response of Square HSS Columns

Square HSS columns exhibit an even greater deviation from the AISC 360 curve than circular sections, as shown in Figure 12b. Across a wide range of slenderness ratios, the unified column curve significantly underestimates buckling strength, with numerical results exceeding AISC predictions by approximately 8–15% in the inelastic buckling range. The separation between the SHS curves and the AISC curve is more pronounced than for CHS columns and remains evident until the elastic buckling regime is reached.

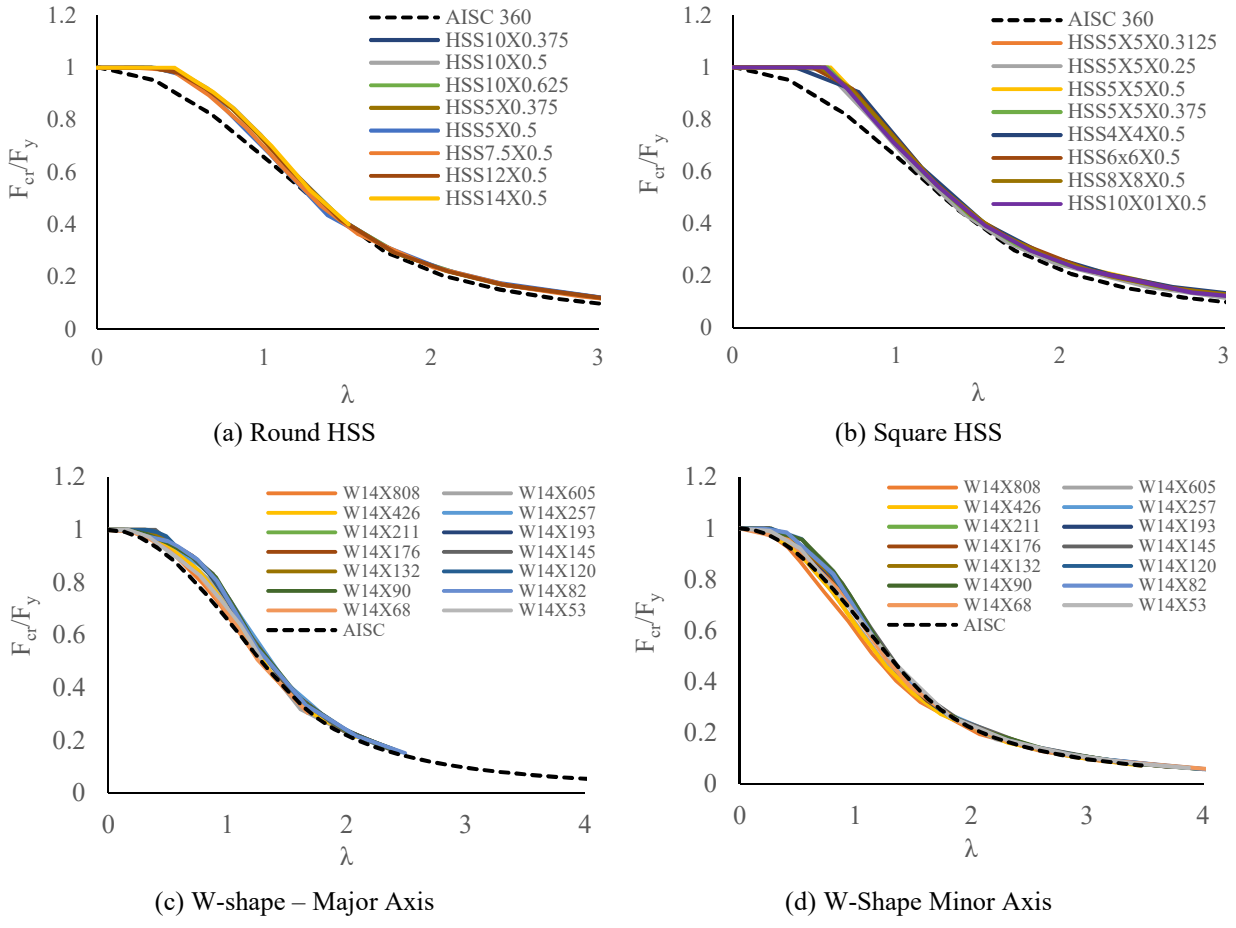

Figure 12: Normalized flexural buckling curves for high-strength steel columns: (a) CHS, (b) SHS, (c) W-shape major-axis buckling, and (d) W-shape minor-axis buckling, compared with the AISC 360-22 unified column curve.

Despite the lack of full geometric symmetry relative to CHS members, SHS columns benefit from closed-section action, which provides enhanced flexural stiffness and reduced imperfection

sensitivity compared to open W-shapes. While the presence of flat walls and corner regions introduces localized stress concentrations, these effects do not appear to negate the overall stability advantages of closed sections. Consequently, SHS columns demonstrate the highest normalized buckling strengths among the section types considered, with relatively modest variation across the range of width-to-thickness ratios examined.

4.3 Material Strength Sensitivity of HSS Column Buckling Behavior

To assess whether the observed HSS buckling trends are influenced by the use of high-strength European steel data, a supplementary set of simulations was performed using ASTM A500 Grade C material properties. Figure 13 compares the normalized flexural buckling response of circular and square HSS columns modeled with S700 and A500 Grade C steels against the AISC 360-22 unified column curve.

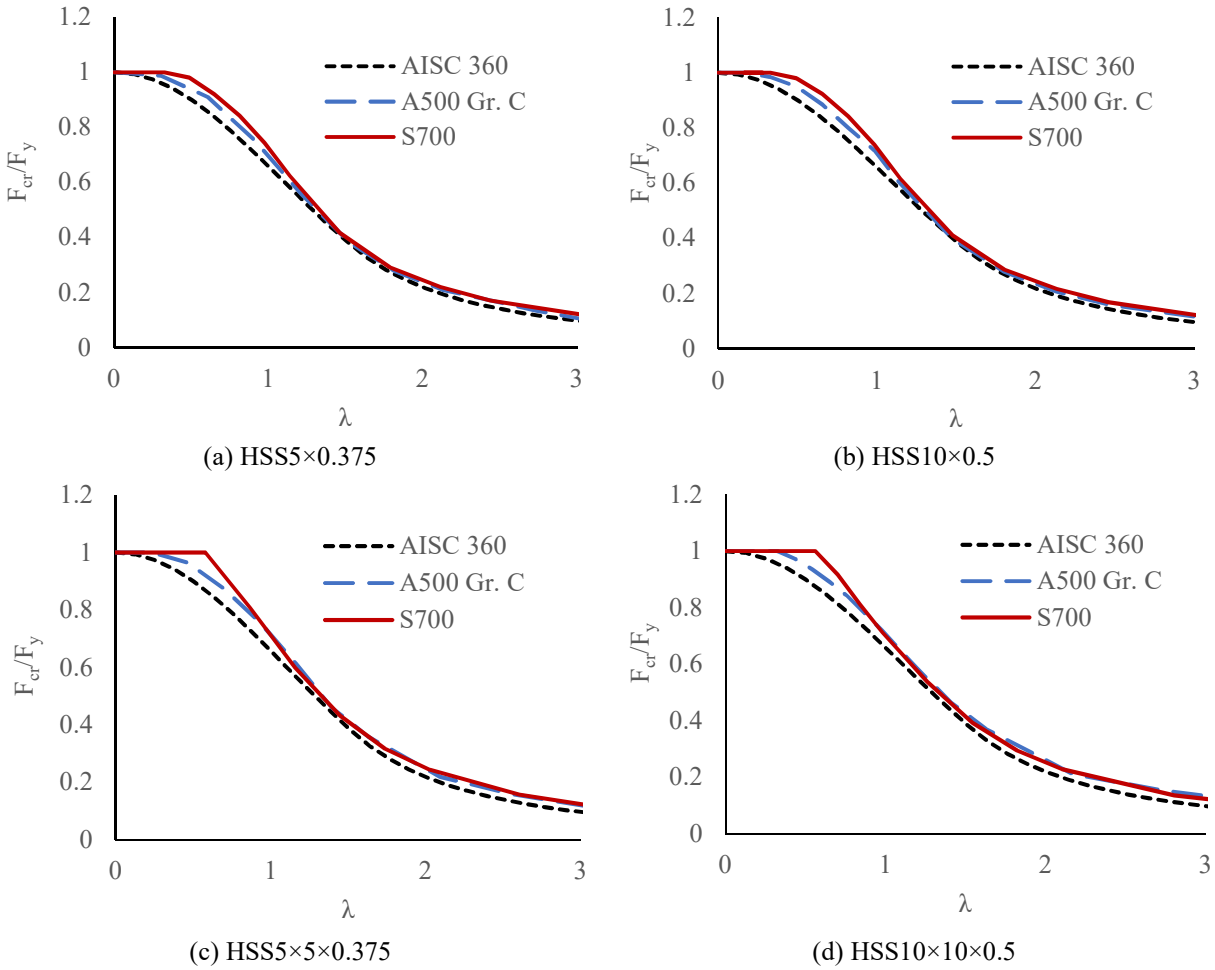

Figure 13: Simulated column flexural buckling curves for HSS columns using S700 and A500 Gr. C steels.

The results indicate that HSS columns exhibit higher inelastic buckling strengths than predicted by the AISC column curve regardless of material strength, confirming that the observed conservatism is primarily attributable to closed-section behavior rather than steel grade. For both materials, square HSS (SHS) members consistently demonstrate larger strength exceedance relative to AISC predictions than circular HSS (CHS), reflecting differences in stiffness

distribution and residual stress characteristics inherent to section geometry. Quantitatively, S700 HSS columns exceed the AISC curve by approximately 8–15% for CHS and 12–20% for SHS across the inelastic slenderness range examined. In comparison, A500 Grade C HSS columns exceed the AISC curve by approximately 5–10% for CHS and 8–15% for SHS. While the S700 sections develop higher absolute buckling strengths due to their increased yield stress, the incremental increase relative to A500 Grade C is modest, generally on the order of 3–6%, and does not alter the qualitative relationship between HSS columns and the AISC design curve.

These findings demonstrate that the conservative bias of the AISC unified column curve for HSS members persists across a range of material strengths, reinforcing the conclusion that current column design provisions - calibrated largely using open-section data - do not fully capture the enhanced buckling performance of closed HSS members. The use of S700 steel therefore does not artificially inflate the observed trends, but rather provides an upper-bound representation of high-strength HSS behavior consistent with that observed for contemporary U.S. HSS materials.

4.4 Comparison with W Shape Columns

Direct comparison of the HSS results with the W shape results shown in Figure 12 reveals a clear hierarchy in buckling performance relative to the AISC 360 curve. W-shape columns buckling about the minor axis exhibit the closest agreement with the AISC curve and, for heavy sections, may even experience slight overprediction in the inelastic range. W-shape columns buckling about the major axis generally exceed the AISC curve by a modest margin, particularly for high-strength steel. In contrast, closed HSS sections exhibit systematically higher normalized buckling strengths, with CHS columns outperforming W shape major-axis buckling and SHS columns exhibiting the greatest deviation from the unified curve. The observed hierarchy can be summarized as:

$$\text{SHS \& RHS} > \text{CHS} \approx \text{W shape (major axis)} > \text{W shape (minor axis)}$$

This hierarchy underscores the dominant role of cross-section geometry in governing high-strength column stability and highlights a key limitation of applying a single unified column curve to both open and closed sections. The HSS results provide strong motivation for shape-specific consideration of high-strength column behavior, consistent with approaches adopted in other design provisions such as AISC 370.

5. Comparative Discussion and Design Implications

The comparative evaluation of W shape and HSS column behavior highlights the strong influence of cross-sectional form on flexural buckling response at high yield strengths. While the unified AISC 360 column curve provides a reasonable baseline for W-shapes, particularly those with moderate geometry and residual stress levels, its conservatism increases markedly for closed-section columns. Closed-section behavior reduces sensitivity to imperfections and residual stresses, leading to higher buckling resistance than implied by a design curve calibrated primarily on open sections. This effect is most pronounced for square HSS columns and is also evident, though to a lesser extent, for circular sections.

These findings are consistent with prior experimental and numerical observations reported in the literature for tubular and box-type columns and align with design philosophies that distinguish between section types. While the present study does not propose revised column curves, the

numerical evidence suggests that the assumption of a single unified column curve may not fully capture the behavior of high-strength steel columns across different cross-sectional forms.

From a design perspective, the results indicate that current provisions may lead to overly conservative designs for high-strength steel columns, particularly in the inelastic buckling regime. The findings provide a quantitative basis for continued discussion within the SSRC and AISC communities regarding whether section-type-dependent considerations may be appropriate for future high-strength steel design provisions.

6. Conclusions

This study examined the flexural buckling behavior of high-strength steel columns using validated nonlinear finite element models incorporating initial geometric imperfections, residual stresses, and nonlinear material behavior. Rolled W-shape columns fabricated from ASTM A992 and ASTM A913 Grade 80 steels, as well as circular and square hollow structural section (HSS) columns modeled using A500 Gr. C and high-strength S700 material properties, were investigated over a broad range of slenderness ratios.

The results indicate that the AISC 360-22 unified column curve provides a generally conservative baseline for rolled W-shape columns, with good agreement in the elastic and yielding regimes. In the inelastic buckling range, the level of conservatism varies with section geometry and buckling axis, particularly for high-strength W-shapes where major-axis buckling strengths often exceed AISC predictions, while minor-axis buckling remains more sensitive to residual stress effects.

High-strength HSS columns exhibit systematically higher normalized buckling strengths than predicted by the unified column curve. Circular HSS columns show moderate conservatism, while square HSS columns exhibit more pronounced deviations across a wide range of slenderness ratios. A clear hierarchy in buckling performance is observed, with square and rectangular HSS columns performing best, followed by circular HSS, W shape major-axis buckling, and W shape minor-axis buckling. Supplementary simulations using ASTM A500 Gr. C material properties confirm that conventional U.S. HSS columns also exceed AISC 360 predictions, indicating that the observed conservatism is primarily associated with closed-section behavior rather than material strength alone. While S700 sections develop higher absolute buckling strengths, the incremental increase relative to A500 Gr. C is modest and does not alter the overall trends.

The HSS results based on S700 material models are intended to identify relative trends in high-strength HSS buckling behavior rather than to imply direct applicability to current U.S. design provisions. Nevertheless, the consistency between S700 and A500 Gr. C results suggests that the use of S700 steel does not artificially inflate the observed response and provides a reasonable upper-bound representation of high-strength HSS behavior.

The findings of this study suggest that while the unified column curve adopted in AISC 360 provides a practical and conservative design approach, cross-sectional geometry plays a significant role in the flexural buckling behavior of high-strength steel columns. The numerical evidence presented herein provides a basis for continued discussion within the SSRC and AISC communities regarding the applicability of unified stability provisions to different high-strength

column section types. Additional experimental data for high-strength W-shape and HSS columns would be valuable for further informing future stability-related design guidance.

Acknowledgments

The authors are grateful to AISC for funding this research and for sharing all the relevant information for this project. However, any opinions presented in this paper are solely those of the authors. The authors also greatly acknowledge the high-strength steel material testing data provided by the producers. The guidance provided by Dr. Devin Huber from AISC throughout the completion of this project is greatly appreciated.

References

AISC (2019), "High Strength Steel," Task Group Report prepared by the AISC Committee on Specifications Ad Hoc Task Group on High Strength Steel, December 19, American Institute of Steel Construction, Chicago, Ill.

AISC (2022), *Specification for Structural Steel Buildings*, ANSI/AISC 360-22, American Institute of Steel Construction, Chicago, Ill.

AISC (2021), *Specification for Structural Stainless-Steel Buildings*, ANSI/AISC 370-21, American Institute of Steel Construction, Chicago, Ill.

Alpsten, G. A. (1968), "Thermal Residual Stresses in Hot-Rolled Steel Members," Fritz Engineering Laboratory Report No. 337.3, Lehigh University, Bethlehem, Pa.

ANSYS (2023), Ansys® Mechanical APDL, Release 2023 R1, Theory Reference, ANSYS, Inc.

Ban, H., Shi, G., Shi, Y., and Bradford, M. A. (2013), "Experimental Investigation of the Overall Buckling Behaviour of 960 Mpa High Strength Steel Columns," *Journal of Constructional Steel Research*, *88*, 256-266

Boissonnade, N., and Somja, H. (2012), "Influence of Imperfections in FEM Modeling of Lateral Torsional Buckling," In *Proceedings of the Annual Stability Conference* (pp. 18-21). Structural Stability Research Council, Grapevine, Texas.

Bjorhovde, R. (1972), "Deterministic and Probabilistic Approaches to the Strength of Steel Columns," PhD thesis. Lehigh University, Bethlehem, Pa.

ECCS Technical Committee 8 (2008), *The Residual Stresses in Hot-Rolled Structural Sections and Their Effect on Column Strength.*

EN 1993-1-1 (2005), *Design of Steel Structures – Part 1.1: General Rules and Rules for Buildings*, CEN - European committee for Standardization, Brussels, Belgium.

Fadden, M., and McCormick, J. (2014), "Finite element model of the cyclic bending behavior of hollow structural sections," *Journal of Constructional Steel Research*, *94*, 64-75.

Ferreira Filho, J. O., Tankova, T., Carvalho, H., Martins, C., and da Silva, L. S. (2022), "Experimental and Numerical Flexural Buckling Resistance of High Strength Steel Columns and Beam-Columns," *Engineering Structures*, *265*, 114414.

Fukumoto, Y., and Itoh, Y. (1983), "Evaluation of Multiple Column Curves Using the Experimental Data-Base Approach," *Journal of Constructional Steel Research*, *3*(3), 2-19.

Galambos, T. V., and Ketter, R. L. (1959), "Columns Under Combined Bending and Thrust," *Journal of the Engineering Mechanics Division*, *85*(2), 1-30.

Huber, A.W. (1956), "The Influence of Residual Stress on The Instability of Columns," Doctoral. Dissertation, University Microfilms, Inc., Ann Arbor, Mich.

Jönsson, J., and Stan, T. C. (2017), "European Column Buckling Curves and Finite Element Modelling Including High Strength Steels," *Journal of Constructional Steel Research*, *128*, 136-151.

Lamarche, C. P., and Tremblay, R. (2011), "Seismically Induced Cyclic Buckling of Steel Columns Including Residual-Stress and Strain-Rate Effects," *Journal of Constructional Steel Research*, *67*, 1401-1410.

Li, G.Q., Wang, Y.Q., and Chen, S.W. (2012), "Experimental Study On The Overall Buckling Behavior Of High Strength Steel Columns," *Journal of Constructional Steel Research*, *74*, 145-150.

Ma, Y., Gardner, L., and Yuan, H. (2015), "Buckling of Ferritic Stainless Steel Members Under Combined Axial Compression and Bending," *Journal of Constructional Steel Research*, *110*, 190-198.

Meng, X., and Gardner, L. (2021). "Flexural buckling of normal and high strength steel CHS column," *Structures*, *34*, 4364-4375.

prEN 1993-1-14 (2020), *Eurocode 3: Design of steel structures–Part 1-14: Design assisted by finite element analysis*, European committee for Standardization, Brussels, Belgium.

Quayyum, S., and Hassan, T. (2017), "Initial Residual Stresses in Hot-Rolled Wide-Flange Shapes: A Computational Technique and Influence on Structural Performances," *Journal of Structural Engineering*, *143*(5), 04017013.

Rasmussen, K.J.R., and Hancock, G.J. (1995), "Tests of High Strength Steel Welded I-Section Columns," *Journal of Constructional Steel Research*, *32*(2), 167-187.

Somodi, B., and Kövesdi, B. (2016), "Flexural Buckling of Cold-Formed High-Strength Steel Rectangular Hollow Section Columns," *Journal of Constructional Steel Research*, *122*, 614-626.

Somodi, B., and Kövesdi, B. (2017), "Flexural Buckling of Welded Box Section Columns Made of High Strength Steels," *Journal of Constructional Steel Research*, *128*, 567-579.

Spoorenberg, R. C., Snijder, H. H., Cajot, L.-G., and May, M. S. (2013), "Experimental Investigation on Residual Stresses inn Heavy Wide Flange QST Steel Sections," *Journal of Constructional Steel Research*, *89*, 63-74.

Stall, K., Culhane, A., Sun, L., Cross, R. C., and Steiner, M. (2024), "Tensile Coupon Testing and Residual Stress Measurements of High-Strength Steel Built-Up I-Shaped Sections," *Engineering Journal*, *61*(3).

Stroetmann, R., and Penner, G. (2024), "Buckling Resistance and Residual Stresses of Welded Box Xolumns Made of High-Strength Steels," *10th International Conference on Steel and Aluminum Structures (ICSAS24)*, Rio de Janeiro, Brazil.

Sun, Y., Liang, Y., and Zhao, O. (2020), "Minor-Axis Flexural Buckling Behaviour and Resistances of Pin-Ended S690 High Strength Steel Welded I-Section Columns," *Thin-Walled Structures*, *156*, 106980.

Voth, A. P., and Packer, J. A. (2012), "Branch plate-to-circular hollow structural section connections. I: Experimental investigation and finite-element modeling," *Journal of Structural Engineering*, *138*(8), 995-1006.

Wang, J., and Gardner, L. (2013), "Testing and Numerical Simulation of High Strength Steel Hollow Sections Under Bending," *Journal of Constructional Steel Research*, *80*, 100-108.

Yin, F., Wang, J., Yang, L., Kang, N., and Elliott, F. (2024). "Testing and design of cold-formed high strength steel square hollow section columns," *Journal of Constructional Steel Research*, *213*, 108394.

Yun, X., Zhu, Y., Meng, X., and Gardner, L. (2023), "Welded Steel I-Section Columns: Residual Stresses, Testing, Simulation and Design," *Engineering structures*, *282*, 115631.

Ziemian, R. D., ed. (2010). *Guide to Stability Design Criteria for Metal Structures*, 6th ed., Structural Stability Research Council, Wiley, New Jersey.